Preprints (www.preprints.org) | NOT PEER-REVIEWED | Posted: 21 March 2023 doi:10.20944/preprints202303.0358.v1

Disclaimer/Publisher's Note: The statements, opinions, and data contained in all publications are solely those of the individual author(s) and contributor(s) and not of MDPI and/or the editor(s). MDPI and/or the editor(s) disclaim responsibility for any injury to people or property resulting from any ideas, methods, instructions, or products referred to in the content.

Article

Gas-Water Characteristics of Tight Sandstone in Different Charging Model in Xihu Sag, East China Sea Basin

Jinlong Chen [a,b], Zhilong Huang [a,b *], Genshun Yao [c] and Hongche Fan [d]

[a] State Key Laboratory of Petroleum Resources and Prospecting, China University of Petroleum (Beijing), Beijing 102249, China;
[b] College of Geosciences, China University of Petroleum, Beijing 102249, China;
[c] Hangzhou Institute of Geology, China National Petroleum Corporation;
[d] Kunlun Digital Technology Co. , Ltd.
* Correspondence: huangzhilong1962@163.com

Abstract: Reservoir in the Central Structural Zone of the Xihu Sag is the Huagang Formation, dominated by natural gas reservoirs, and the reservoir in the Western Slope Zone is the Pinghu Formation, dominated by light oil and wet gas. In this paper, the Gas Drive Water Displacement- Magnetic Resonance Imaging (GWD-MRI) experiments are used to simulate the charging characteristics of the sandstone migration layer. The centrifugal- Magnetic Resonance (Cen-NMR) experiments simulate the short-term fast trap charging process, and the Semi-Permeable Baffle (SPB) charging experiment simulates the slow trap accumulation process. Studies have shown that there is a start-up pressure for the migration layer charging, and the start-up pressure of the core with a permeability of 0.3mD is about 0.6MPa. Experimental simulations have confirmed that there is a front zone with changed water saturation, with a width of about 1-1.5cm. The migration layer charging mainly has two actions, drive effect and carry effect. The drive effect reduces the water saturation to 70%-80%, and the carry effect can still reduce the water saturation by 5%-10%. The water saturation of rapid charging is mainly affected by the petro-physical. The porosity is high, the water saturation is low. The water saturation decreased significantly with the increase of centrifugal force when the centrifugal force is smaller. If the centrifugal force is greater than 0.8 MPa, the water saturation decreases slowly. The water saturation of the trap slowly charging is basically maintained at 40%-50%, which matches the water saturation of the airtight coring from 40%-55%, the petro-physical do not affect the final water saturation.

Keywords: gas drive water displacement; Magnetic Resonance Imaging; Semi-Permeable Baffle; centrifugal-NMR; start-up pressure

1. Introduction

There are many articles have study gas charging and physical modeling (Zheng, 2016; Wang, 2018; Li, 2019; Masri, 2021), mainly according to the actual situation to design the driving fluid and displacement conditions, the core plunger is subjected to displacement experiments, and numerical simulations are carried out according to the experimental results. Some scholars have also conducted visualization studies of displacement experiments. Lysova(2011) has analysis the residual water depend on Magnetic Resonance Imaging(MRI) experiment of natural gas charging (Lysova, 2011), and some scholars placed CT imaging devices on the core displacement chamber (Masri , 2021) to analyze the changes in different parts of water saturation after displacement. According to centrifugal-NMR experiments, there are many articles on the distribution of core residual water (Arogun, 2011; Daigle, 2015; Shao, 2017; Chen, 2019). The fluidity of the reservoir fluid can be analyzed according to the centrifugal force. Semi-Permeable Baffle experiments are mostly used in material research (Niroomand, 2019; Gu, 2020). The Semi-Permeable experiments of porous materials are similar to geological samples, and the wettability of

© 2023 by the author(s). Distributed under a Creative Commons CC BY license.

Preprints (www.preprints.org) | NOT PEER-REVIEWED | Posted: 21 March 2023 doi:10.20944/preprints202303.0358.v1

porous materials is studied (Feng, 2019), it has reference significance with the wettability of rock samples.

The Centrifugal- Nuclear Magnetic Resonance (Cen-NMR) experiment uses different speeds to centrifuge the core, so that the water in the pores is driven out of the core under the action of centrifugal force. Generally, the speed is mainly from 1000rpm to 10000rpm, and the centrifugal force produced is mainly 0.1-5MPa. After centrifugation, the samples are tested by NMR spectroscopy and weighed at the same time, to analyze the water content and water-bearing pore distribution characteristics under different centrifugal force conditions (Shao, 2017; Chen, 2019). Generally, the water content is stable in a smaller range when the speed is around 6000-8000rpm. The water saturation after centrifugation has a wide range, generally from 80% to 20%. For medium-coarse sandstone, the water saturation after centrifugation is as low as 10%.

The Semi-Permeable Baffle (SPB) experiment mainly uses a ceramic baffle that only allows the liquid phase to pass through at the end of the core which used to measure capillary data. Fill the core chamber with natural gas at a certain pressure, and the natural gas will drive out the water in the core under the action of pressure. The driven liquid phase enters the measuring cup through the semi-permeable ceramic plate, while the gas phase is still filled in the core chamber (SY/T 5346-2005). Due to experimental conditions, the gas chamber pressure is generally 0~1MPa, the experiment equilibrium time is very long, and equilibrium time is generally >6h generally, which mainly simulates low pressure trap charging. It is generally believed that the Semi-Permeable Baffle experiment is more in line with the actual trap charging environment, and the water saturation varies from 90% to 50%.

Gas drive water displacement- Magnetic Resonance Imaging (GWD-MRI) experiment uses a displacement device combined with a Magnetic Resonance Imaging (MRI) device. According to the design, the core driving experiment can complete the simulation of different driving pressures, different driving times, and different types of fluid. Under the gas drive water model, the driving pressure depends on the core petro-physical to select the appropriate displacement pressure of 0-5MPa, the driving time 1-48h is appropriately selected. But the visualization of the displacement process is difficult to complete. In order to visualize the drive process, this paper uses the technical method of combining drive device and the Magnetic Resonance Imaging (MRI) device. Generally, the driving pressure of fine sandstone is generally 0~1MPa. If the current driving pressure cannot drive water out, increase the driving pressure or increase the driving time. After driving for a period of time, perform Magnetic Resonance Imaging (MRI) analysis to obtain residual fluid distribution characteristics (Lysova, 2011).

The three types of natural gas charging simulation experiments have their own characteristics. The Cen-NMR experiment takes short time, has a large driving pressure range, and can analyze the residual water distribution, which is suitable for analyzing the characteristics of short-term high-intensity charging. The Semi-Permeable Baffle has a long experiment time and low driving pressure, this experiment condition can better simulate the charging process in the underground trap, and the final water saturation is match with the current water saturation of most gas fields. GWD-MRI can observe the spatial distribution characteristics of its residual water. Gas drive water is generally under low pressure conditions. During the driving process, the end of the core will discharge water and gas at the same time, so the core driving experiment can better reflect the charging passage of the transport system. Combining the three types of experiments can analyze short-term high-intensity trap charging, slowly trap charging, and migration layer charging.

2. Samples and Experiment

2.1. Sample Information

The study area is located in the Xihu Sag of the East China Sea Basin. The East China Sea Basin is a large offshore basin located off Shanghai and north of Taiwan Island, China. The Xihu Sag is located in the central part of the East China Sea Basin. It is about 350km

Preprints (www.preprints.org) | NOT PEER-REVIEWED | Posted: 21 March 2023 doi:10.20944/preprints202303.0358.v1

north-south and about 150km east-west. The depression area is about 50,000 square kilometers. From west to east, the Xihu Sag consists of the Western Slope Zone, the Central Tectonic Overturning Zone, and the Eastern Uplift Zone. At present, the exploration areas are the central and southern parts of the central structural zone, and the central part of the western slope zone. The core samples selected in this paper contain a total of 5 wells, of which 4 are located in the central tectonic overturning zone and one is located in the western slope zone (Figure 1).

The main reservoir in the western slope zone is the Pinghu Formation (E2P), which is a bay-tidal platform deposit. The main lithology is dark mudstone, coal rock, and fine sandstone. The main reservoir in the central tectonic overturning zone is the Huagang Formation (E3h), which is a river-lacustrine deposit, and the main lithology is thick fine sandstone and mudstone.

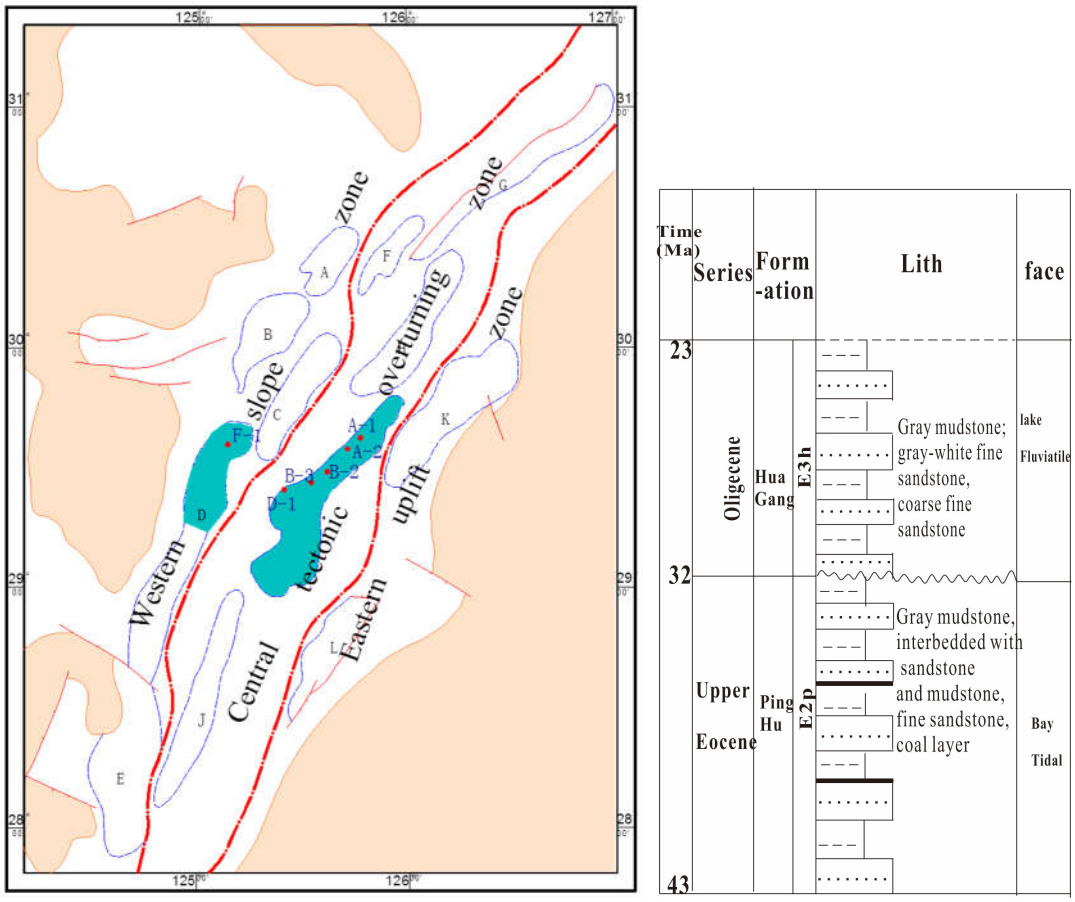

Figure 1. Location and strata of the study area in Xihu Sag.

Select 10 samples from the Xihu Sag, including 9 cores from the Huagang Formation in the Central Tectonic Zone and 1 core from the Pinghu Formation in the Western Slope Zone. The complete plunger sample has a diameter of 2.5cm and a length of 4-5cm. The core porosity and permeability are measured first. Select 3 cores for vacuum-pressurization saturation, generally vacuum 4-6h, water pressure 30MPa, and saturation time generally 24h. The water-saturated core is analyzed by the GWD-MRI combined detection instrument, and the driving pressure is set to 0.3MPa, 0.5MPa, 0.8MPa, 1MPa, and the driving time varies from 1 min to 10 min. When a displacement is completed, the T2 relaxation time is measured and MRI is performed. An MRI is about 40 minutes. After the GWD-MRI is completed, the sample is dried and re-saturated with water. And then, 7 cores were selected for vacuum-pressurization saturation, and the saturated cores were subjected to Cen-NMR experiments to detect water saturation changes under different centrifugal force conditions. The centrifugal speed was 1500-7000rpm, and the corresponding centrifugal force was 0.1-2.2MPa. At last, 6 samples were selected for the Semi-

Preprints (www.preprints.org) | NOT PEER-REVIEWED | Posted: 21 March 2023 doi:10.20944/preprints202303.0358.v1

Permeable Baffle (SPB) experiment. The natural gas driving pressure was set to 0-1.4MPa, and each pressure point needed to wait for the discharge of water to stabilize before it could be recorded.

Table 1. Information of samples.

NO.	Well	Formation	depth	Lithology	Length	Diameter	Pore %	Permeabilty mD	SPB	GWD-MRI	Cen-NMR
A1	A-1	H3	3449	Fine sandstone	3.71	2.47	7.6	0.091	√		√
A4	A-1	H4	3823.1	Fine sandstone	4.07	2.47	11.2	1.946	√		
A5	A-1	H4	3831.6	Fine sandstone	3.64	2.47	10.6	1.018			√
A7	A-2	H3	3614.9	Fine sandstone	3.53	2.47	10	8.152	√		√
A10	A-2	H6	4320.9	Fine sandstone	3.36	2.48	8	0.344		√	√
A17	B-2	H3b	3752.7	Fine sandstone	4.03	2.51	10.7	2.623	√		
A20	B-2	H4b	4008	Fine sandstone	4.07	2.47	7.5	0.291	√		
A25	D-1	H3	4324.9	Fine sandstone	3.47	2.49	8.2	1.394		√	√
A26	D-1	H8	5106.9	Fine sandstone	3.39	2.47	8.5	0.369	√		√
A45	F-1	P10	4106.86	sandstone	3.05	2.49	12.5	5.292		√	√

2.2. Experiment

(1) Gas drive water displacement - Magnetic Resonance Imaging (GWD-MRI)

Displacement-nuclear magnetic resonance imaging combined equipment can be used to visualize the distribution of formation water during the displacement process. The displacement instrument uses the MR-HTHP type high temperature and high pressure displacement device. The confining pressure of the holder is 0~30MPa, and the driving pressure is 0~5MPa. Magnetic imaging is detected by MacroMR12-150H nuclear magnetic resonance instrument. The diameter of the coil is 150mm, which can form a stable magnetic field in the area of 100mm, the frequency is 12.80MHz, the magnet strength is 0.3T, and the imaging time is about 40min each time. The displacement needs to be stopped during the imaging process. The nuclear magnetic resonance imaging (MRI) instrument can also perform NMR T2 spectrum detection at the same time, the echo interval is set to 0.15ms, the measurement time is 8000ms, and the CPMG sequence (Glorioso, 2003) can be used for quantitative evaluation of water content (Figure 2).

Preprints (www.preprints.org) | NOT PEER-REVIEWED | Posted: 21 March 2023 doi:10.20944/preprints202303.0358.v1

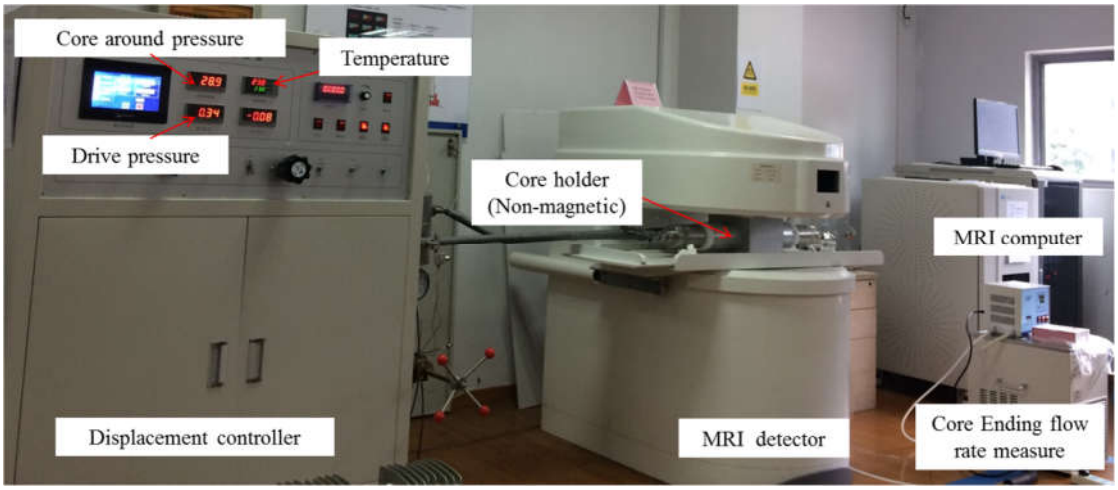

Figure 2. Displacement-nuclear magnetic imaging experimental device.

(2) Semi-Permeable Baffle (SPB) charging experiment

Use a semi-permeable baffle that only allows water to pass through but cannot allow natural gas to pass through as the compartment of the displacement chamber. When natural gas exists in the high pressure chamber, the natural gas enters the core under the action of gas pressure, and discharges a part of the water. Water seeps out into the measure cup through the semi-permeable baffle, while the natural gas will not escape from high pressure chamber, thus simulating the accumulation characteristics of the reservoir. The instrument uses the GMD-III type high temperature and high pressure capillary pressure resistivity continuous measuring instrument, the driving pressure is 0~1.4MPa, the pressure stability accuracy is 0.01MPa, and the formation water volume measurement accuracy is 0.005ml.

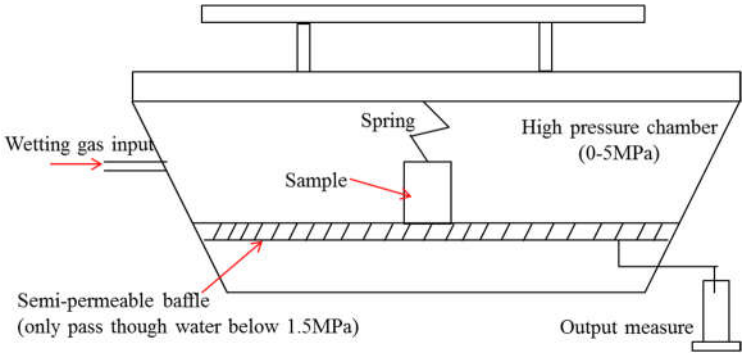

Figure 3. Semi-permeable baffle experiment device (SYT 5346-2005 industry standard).

(3) Centrifugal- Nuclear Magnetic Resonance (Cen-NMR) experiment

NMR is detected by MacroMR12-150H, frequency is 12.80MHz, magnet strength is 0.3T, coil diameter is 150mm, echo interval is set to 0.15ms, measurement time is 8000ms, CPMG sequence (Glorioso, 2003) is used, same as MRI device in figure 2. Water saturating uses the vacuum-pressurization saturation, which vacuum 4-6h, water pressure 30MPa, and saturation time 24h. The centrifugal speed is generally 1500r/min, 3000r/min, 4000r/min, and the maximum centrifugal speed is 7000r/min.

3. Result

Displacement-MRI is mainly used to analyze the characteristics of gas passage in the migration layer, semi-permeable baffle are mainly used to analyze the charging characteristics in traps, and centrifugal-NMR is mainly used to analyze short-term charging characteristics.

Preprints (www.preprints.org) | NOT PEER-REVIEWED | Posted: 21 March 2023 doi:10.20944/preprints202303.0358.v1

3.1. migration layer charging result

The main feature of the migration layer charging is that, the natural gas and the formation water are discharged from the formation together, the gas is mainly passing through the core, and the displacement experiment is most fit with the characteristics of the migration layer charging. This paper analysis the Nuclear Magnetic Resonance Imaging (MRI) while Gas driven Water Displacement (GWD), and completes 3 samples. The driving pressure is 0~2MPa, the total displacement time is 60~90min, and each displacement time is 1~10min. After one displacement is completed, weighing and MRI are carried out, and one single MRI is about 40 minutes, NMR T2 spectrum detection at the same time.

(1) Sample A10 experiment result

A sample of A10 (4320.9m from Well A-2) has a permeability of 0.34mD and a porosity of 8%. After a drive pressure of 0.3MPa for 5 minutes and a drive pressure of 0.6MPa for 20 minutes, the cumulative driving time is 25 minutes, Nuclear Magnetic Imaging (MRI) shows that the residual water is evenly distributed, indicating that natural gas cannot charge low-permeability cores under the condition of 0.6MPa. After 0.3MPa and 0.6MPa driving, the water saturation of the samples decreased, which is believed to be the result of water evaporation caused by the heating of the core within 40 minutes of imaging.

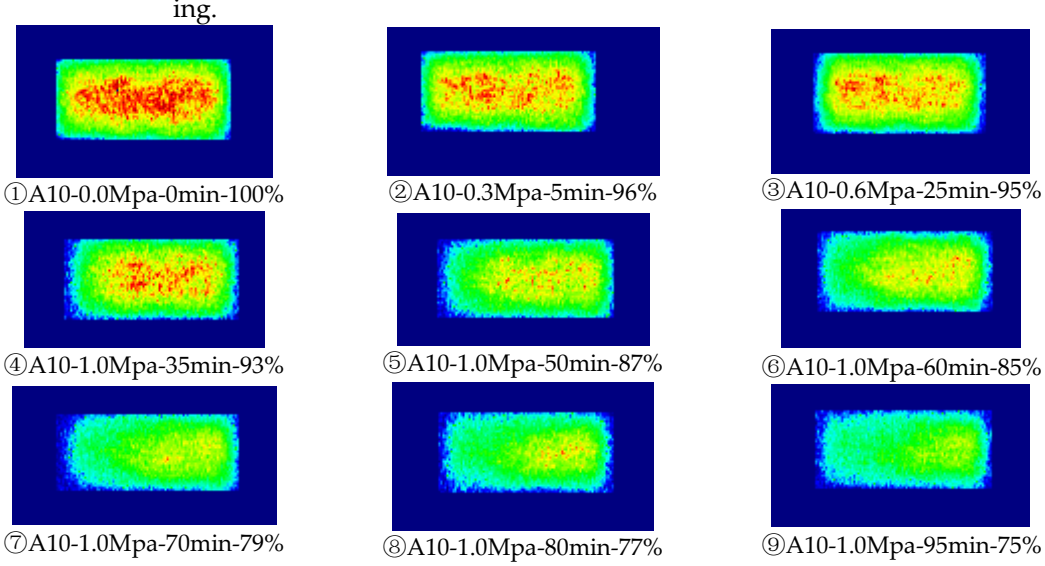

Figure 4. sample of A10 (4320.9m in Well A-2) low-permeability GWD-MRI experiment results.

The name of the photo represents "Sample Number-Driving Pressure-Cumulative Driving Time-Water Saturation"

The drive pressure increased to 1MPa for 10 minutes, the cumulative driving time was 35 minutes. The water content in the front of the core is decreased, the center and the end of the core did not change, and the water saturation was 93%, indicating that 1MPa can charge into the core. Continue to use 1MPa driving pressure for 15 minutes, the cumulative driving time is 50 minutes, water content in the front of the core continues to decrease, and the water content in the center and end of the core begins to decrease, with a water saturation of 87%; cumulative driving time is 60min, 70min, 80min, water content of different core positions all decreased; the cumulative driving time was 95 minutes, the water content at the front of the core was very low, and the water content at the end of the core also decreased significantly, with a water saturation of 75%.

(2) Sample A25 experiment result

The sample of A25 (4324.9m from Well D-1) has a permeability of 1.39mD and a porosity of 8.2%, was tested with one only driving pressure of 0.3MPa. After 5 minutes of driven, the water content in the front of the core decreased significantly, and the water content in the center and the end of the core began to decrease, with a water saturation of

Preprints (www.preprints.org) | NOT PEER-REVIEWED | Posted: 21 March 2023 doi:10.20944/preprints202303.0358.v1

93%, indicating that 0.3MPa can charge into a medium-permeability core. Continue driving for 5 minutes, that is, the cumulative driving time is 10 minutes. The water content in the center and the end of the core decreases slowly, and the water content of the front end of the core decreases significantly, with a water saturation of 87%. The water content at the end of the core is similar to that of the original sample, but the water content in the center and the front of the core has decreased significantly, reflecting that the natural gas has driven the water at the front of the core to the end of the core. When the cumulative driving time 25 minutes, the water content of the core is equal, indicating that the natural gas has completely passed through the core, displacing most of the movable fluid, and the water saturation is 74% at this time. Continuing to use 0.3MPa for driving, the water content of the whole core is decreases, indicating that natural gas can still carry fluid away from the core. The cumulative driving time is 50 minutes, and the water saturation is 71%.

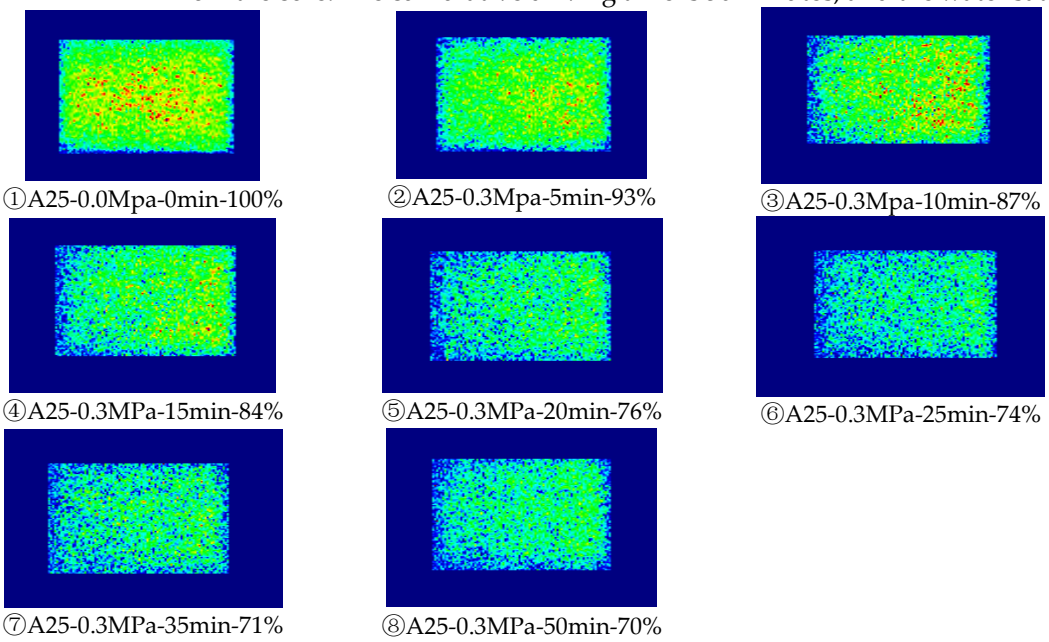

Figure 5. sample of A25 (4324.9m in Well D-1) middle-permeability GWD-MRI experiment results.

The name of the photo represents "Sample Number-Driving Pressure-Cumulative Driving Time-Water Saturation"

(3)Sample A45 experiment result

The sample of A45 (4106.86m from Well F-1) was displaced with a driven pressure of up to 3MPa. Using 0.3MPa to driving for 1 minute, the residual water content of the core was evenly distributed, the water saturation decreased to 86%, reflecting that natural gas quickly passed through the core and displacing the movable water. Continue to use 0.3MPa pressure for 1min, 2min, 11min, that is, the cumulative driving time is 15min, the core water saturation is 76%, and the water saturation is equally and decreases slowly, reflecting the carry effect as the main displacement method. Subsequently, the driving pressure was gradually increased to 3MPa, simple calculation, 0.3MPa driving for 10min, 0.5MPa driving for 5min, 0.8MPa driving for 10min, 1MPa driving for 5min, 2MPa driving for 10min, 3MPa driving for 5min, the water saturation decreases of 4%, 1%, 4%, 2%, 7%, and 2% respectively, indicating that the decrease of water saturation caused by the carry effect is related to the gas flow rate. At same time, high driving pressure also can displace smaller pore water, but drive effect not directly observable.

Preprints (www.preprints.org) | NOT PEER-REVIEWED | Posted: 21 March 2023 doi:10.20944/preprints202303.0358.v1

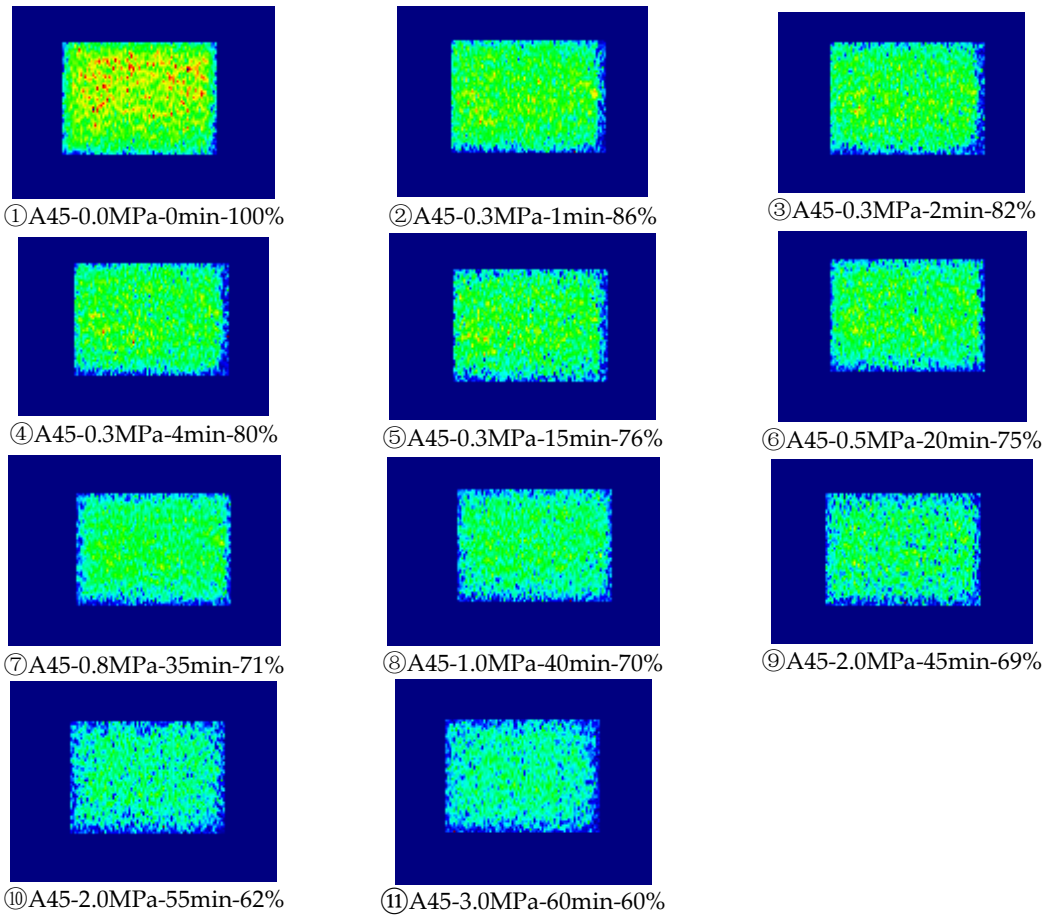

Figure 6. sample of A45 (4106.86m in Well F-1) high-permeability GWD-MRI experiment results.

The name of the photo represents "Sample Number-Driving Pressure-Cumulative Driving Time-Water Saturation"

After completing the MRI of the three samples with different driving times, the NMR T2 spectrum test was still carried out. It can be seen from the T2 spectrum that the T2 relaxation time of the movable fluid in the core is mainly 10~500ms, and the bound water is mainly <10ms. The movable fluid gradually decreases during the driving process, but does not completely displaced. There is no change in bound water. Under the condition of low-pressure driving for 60 to 90 minutes, the water content of low-permeability cores is generally decrease less than 25%, the water content of medium-permeability cores is decrease about 30%, and the water content of high-permeability cores is decrease 40%. The NMR T2 spectrum also shows that a small part of the movable fluid is still stay in the core. According to the equal distribution of water content in the MRI analysis, the remaining movable fluid will decrease by carry effect of flooding gas.

According to the relationship between water saturation and driving time (Figure 7d), the A25 sample is the carry effect during 20-6min, and the water saturation slowly decreases by about 10%. The A10 sample 70-95min is the carry effect, water saturation decrease slowly by 5%. According to trend line analysis, carry effect can make the water saturation drop by 10-15%.

Preprints (www.preprints.org) | NOT PEER-REVIEWED | Posted: 21 March 2023 doi:10.20944/preprints202303.0358.v1

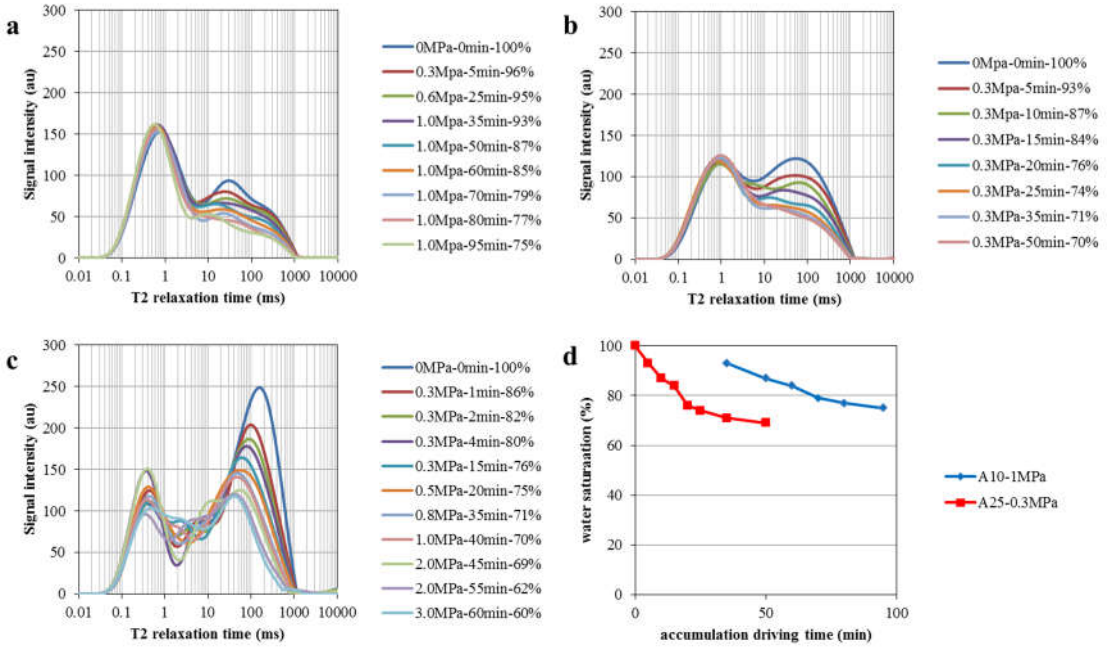

Figure 7. T2 spectrum and water saturation changes after displacement. a: T2 spectrum of A10 after different drive time; b: T2 spectrum of A25 after different drive time; c: T2 spectrum of A45 after different drive time; d: change of Sw with increase of drive time under same pressure

3.2. Trap slowly charge result

The main feature of trap charging is that natural gas will not go away, only water can discharge, which is most fit with the Semi-Permeable Baffle (SPB) charging modeling. This paper has completed the SPB charging experiment of 6 core samples, and the charging pressure is 0~1.4MPa, the balance time of each pressure is 4~6h.

After analyzing of 6 samples, we deem that the water saturation change is almost not affected by the rock physical properties. The water saturation of different cores decreases is basically the same, under the increase of charging pressure, but the rock physical properties affect the final water saturation. Sample of A1 (3449m, Well A-1) has a permeability of 0.1mD, a porosity of 7.6%, and a water saturation of 55% at a charging pressure of 1MPa. If the charging pressure is increased again, the water saturation will not decrease and remains at 50% stably. Samples of A20 (4008m, Well B-2) and A26 (5106.9m, Well D-1), the permeability is 0.29mD and 0.37mD, the porosity is 7.2% and 8.5%, respectively. Charging pressure higher than 1.2MPa, the water saturation is basically unchanged and remains at 45%. Samples A4 (3823.1m, Well A-1), A7 (3614.9m, Well A-2) and A17 (3752.7m, Well B-2), the permeability is 1.9mD, 8.1mD, and 2.6mD, respectively, and water saturation after 1.1MPa is basically unchanged, stable at about 40%. The final water saturation of high porosity and permeability cores will remain at 40%, and low permeability cores will basically remain around 45%-50%.

Preprints (www.preprints.org) | NOT PEER-REVIEWED | Posted: 21 March 2023 doi:10.20944/preprints202303.0358.v1

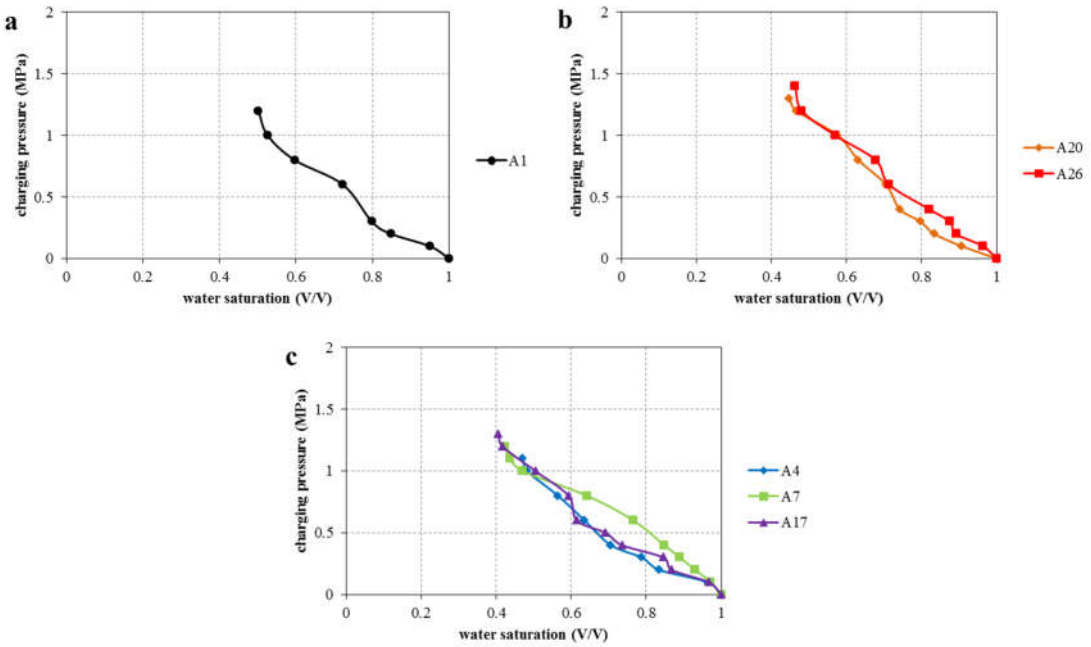

Figure 8. Relationship between the charging pressure and the water saturation of SPB experiment. a: Sw change of SPB charging modeling of ultra-low permeability (<0.1mD); b: Sw change of SPB charging modeling of lower permeability (0.1-0.5mD); c: Sw change of SPB charging modeling of middle and higher permeability (>0.5mD).

3.3. Trap rapidly charge result

The main characteristic of short-term high-intensity charge is that the charging pressure is extremely high and the time is relatively short, which is most fit with the centrifugal experiment. Select 7 samples to complete the centrifugal experiments at 1500, 3000, 4000, 5000, 6000, 6500, and 7000 rpm. After each centrifugation is completed, the NMR T2 spectrum test is performed. According to the speed, the length of the centrifugal arm, and the length of the core, the centrifugal speed can be converted into the pressure at the bottom of the core.

$$P_c = 1.097 \times 10^{-9} \Delta\rho L(R_e - \frac{L}{2})n^2 \quad (1)$$

Where, Pc is the centrifugal charge pressure, MPa; Δρ is the density difference between the two fluids, g/cm^3; L is the core length, cm; Re is the max radius of the core, cm; n is the centrifugal rotation speed, rpm.

Converting the centrifugal speed to the pressure at the bottom of the core, it can be seen that, A7, A25, and A45 have the permeability of >2.5mD, when the centrifugal pressure less than 0.6MPa, water saturation rapid decrease, if the pressure is above 0.6MPa, the water saturation decrease slowly, and the water saturation is considered to be Stable at 15%~30%. Samples of A5, A10, and A26 have permeability of 0.3~1mD, when the pressure bigger than 1 MPa, the water saturation decrease slowly. According to curve extension, it is considered that the water saturation is stable at about 30%. The permeability of the A1 sample is 0.1mD. Under the experimental conditions, there is no inflection point for the decrease of water saturation. The residual water saturation at the same pressure is higher than other samples. This reflects that, the inflection point of water decrease influent by core permeability, physical properties is better, inflection point is lower.

Preprints (www.preprints.org) | NOT PEER-REVIEWED | Posted: 21 March 2023 doi:10.20944/preprints202303.0358.v1

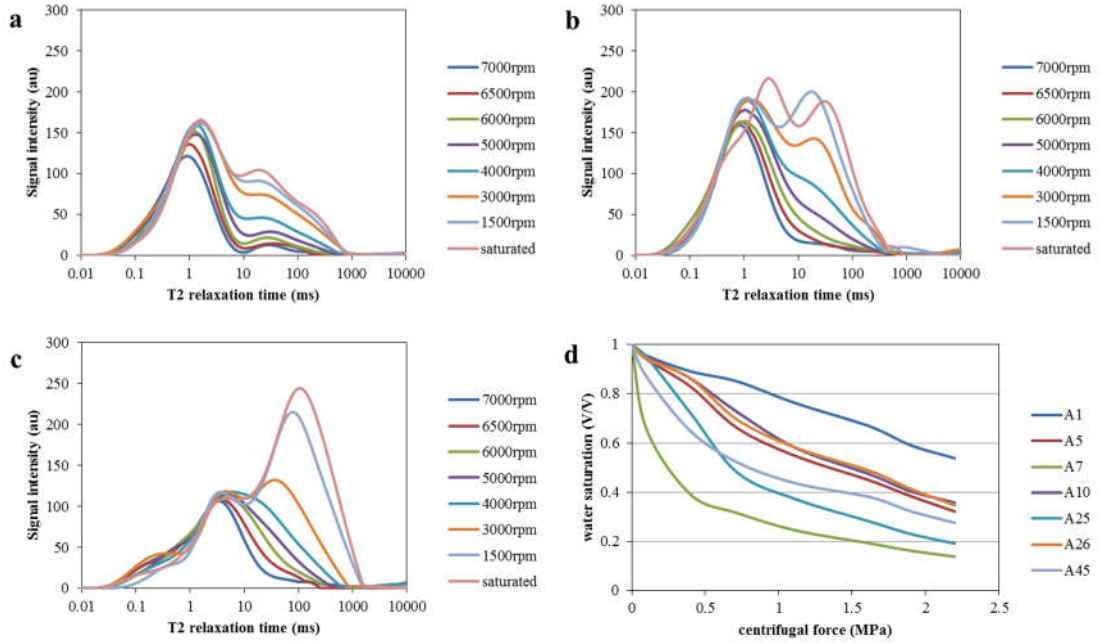

Figure 9. Cen-NMR T2 spectrum and water saturation relationship. a; T2 spectrum of A26 under different rotating speed; b: T2 spectrum of A5 under different rotating speed; c: T2 spectrum of A45 under different rotating speed; d: water saturation change of different centrifugal force.

4. Discussion

4.1. Final water saturation of different physical modeling

The final water saturation of cores with different physical properties is quite different on several experiments. For cores with permeability <0.1mD, there is only one sample of A1. The Semi-Permeable Baffle (SPB) and the Cen-NMR experiment have been completed, but the MRI has not been completed. As the same driving pressure for the ultra-low permeability samples, the water saturation of the SPB modeling is low, and the Cen-NMR is higher.

The sample with a permeability of 0.1-0.5mD represents that there are 3 cores A10, A20, and A26 in total. Among them, the A10 sample completed the GWD-MRI and Cen-NMR experiments, and the A20 sample, with similar properties, completed the SPB experiment. The final water saturation of the SPB experiment of low permeability samples was the lowest, Cen-NMR was medium, and the GWD-MRI was the highest.

The samples with permeability 0.5-2mD represent cores with A4 and A25. A25 completes GWD-NMR and Cen-NMR experiments, and A4 samples with similar permeability complete SPB experiments. The water saturation of Semi-Permeable Baffle, Centrifugal-NMR, and Gas Drive Water Displacement - Nuclear Magnetic Imaging of medium permeability samples are relatively similar.

The samples with permeability> 2mD are A7, A17, and A45. Among them, the A45 sample has completed the GWD-MRI and Cen-NMR experiment, A7 sample with the similar permeability has completed the SPB. Displacement Imaging has the highest water saturation, and the final water saturation of SPB and Cen-NMR is relatively close.

Preprints (www.preprints.org) | NOT PEER-REVIEWED | Posted: 21 March 2023 doi:10.20944/preprints202303.0358.v1

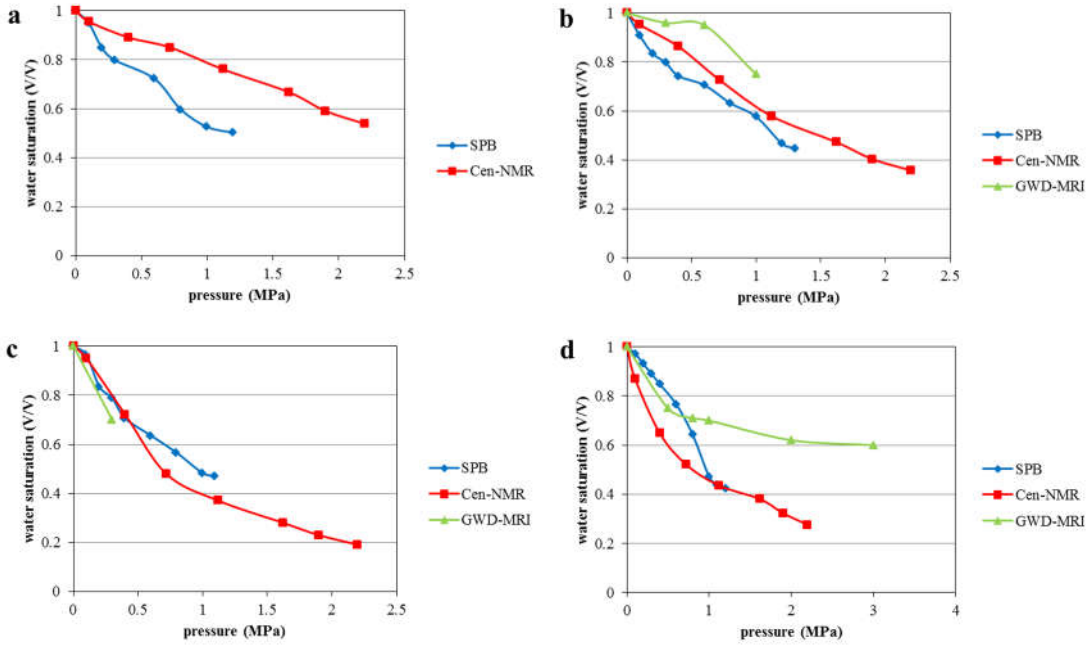

Figure 10. Comparison of water saturation of different modeling experiments. a: comparison of ultra-low permeability(<0.1mD); b, comparison of lower permeability (0.1-0.5mD) c: comparison of middle permeability (0.5-2mD); d: comparison of higher permeability (>2mD).

The water saturation of displacement imaging is generally 10% higher than that of Semi-Permeable Baffle and Centrifugal-NMR modeling under the same driving pressure (Figure 10 b d), indicating that the gas charging of the migration layer is wicker than that of the reservoir within the trap. Permeability> 0.1mD, Semi-Permeable Baffle and Centrifugal Nuclear Magnetic water saturation are relatively similar (Figure 10 b c d), indicating that trap charging have similar water saturation when drive pressure is low(not consider the charging time).

4.2. Characters of charging pass in migration layer

(1) Start-up press gradient

An important feature of the migration layer charging pass is that there is a start-up pressure gradient. When the driving pressure gradient is lower than the starting pressure gradient, the natural gas cannot drive the formation water. Only when the driving pressure gradient is greater than the start-up pressure gradient, the natural gas can drive the formation water. The water saturation of the A10 is basically unchanged at the driving pressures of 0.3 MPa and 0.6 MPa. When the driving pressure is 1 MPa, the water saturation begins to decrease. After the experiment is completed, the final water saturation of 1 MPa is 75% (Figure 10 b). The samples of A25 and A45 have higher permeability, no start-up pressure gradient was found during the physical modeling. Basically for a migration layer of about 0.3mD, the starting pressure is about 0.6MPa (Figure 10 b, slot of displacement imaging), the core length is 3.47cm, and the starting pressure gradient is 0.17MPa/cm. Some scholars have also found that there is a start-up pressure gradient in the oil drive water displacement experiment (Zheng, 2016), and the start-up pressure gradient of oil drive water is relatively high. Generally, for a 0.1mD core, the start pressure is about 0.6-1 MPa/cm (Zheng, 2016), which is affected by oil viscosity. This physical modeling experiment believes that when the permeability is greater than 1mD, the start-up pressure gradient cannot be observed.

(2) Driving front

Simulation experiments show that the charging front of the migration layer is basically a flat (Figure 4 ④ ⑤ ⑥, Figure 5 ② ③ ④). Some scholars believe that the charging is branch-like (liu, 2009), but the core displacement-imaging experiment cannot prove

Preprints (www.preprints.org) | NOT PEER-REVIEWED | Posted: 21 March 2023 doi:10.20944/preprints202303.0358.v1

whether the charge is branch-like or not. It supports that the driving front has a flat with gradual changes in water saturation. When the A10 sample is driving for 60 minutes, with the driving pressure is 1 MPa, and the core is still divided into three sections, the complete displacement section (the left 1/3 of Figure 4 ⑥), the driving front (the middle 1/3 of Figure 4 ⑥), and the unchanged section. (Right 1/3 of Figure 4 ⑥), the core length is 3.36cm, and the driving front is about 1-1.5cm. When the A25 sample was driving for 5 min under the condition of 0.3 MPa, according to the MRI results, the core can be divided into 3 sections, complete displacement section (Figure 5 ②left 1/3), driving front (Figure 5 ②middle 1/3), none change section (the right 1/3 in Figure 5 ②), the core length is 3.47 cm, and the driving front is about 1-1.5 cm. Physical modeling experiments show that the core driving front is about 1-1.5 cm. It is considered that the gas drive water displacement is approximately planar (Figure 11). Completely displaced area is mainly dominated by the residual water of the water film, the driving front is dominated by the gradual decrease of movable water, and the unchanged section is basically full of water. In the physical modeling, due to the small core section, no obvious rock heterogeneity affects the charging of the migration layer.

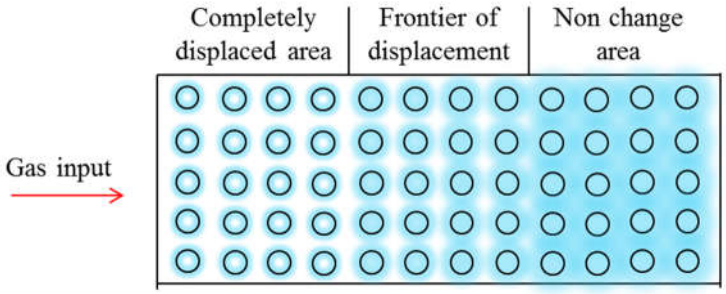

Figure 11. Water content map of core during driving process.

(3) Carry effect

After the natural gas completely go through the entire core, while the displacement pressure remains unchanged, and the water saturation still decreases (Figure 5 ⑤⑥⑦⑧, Figure 6 ②③④⑤). The modeling experiment proves that the gas charging of the migration layer is influent by carry effect by the flooding gas, which the feature is water content decrease in the entire core. The representative image is A25 sample ⑤-⑧ in Figure 5. The core driving pressure is 0.3MPa, and the water saturation of the core has dropped from 76% to 70%. The MRI shows that the water content has dropped uniformly everywhere in the core. Similarly, the A45 sample ②-⑤ in Figure 6 has a driving pressure of 0.3 MPa and a water saturation from 86% to 76%,and the MRI shows that the water content of the core decreases uniformly.

According to the analysis of modeling experiments, the carry effect should not be ignored, and the carry effect will reduce the water saturation by about 10% (Figure 7 d). According to the water saturation change plot in Figure 7d, when the driving time is 20 minutes of A25 sample, the natural gas completely go through the core, and the water saturation is 76% at this time. As the driving continues to 50 minutes, the core water saturation slowly drops to 70%. According to the trend of water saturation, there is still room for further decline. Under the condition of the driving pressure of 0.3MPa, the final water saturation is expected to be around 60%-65%, that is, the carry effect can reduce the water saturation by about 10%-15%.

After the natural gas go pass the entire core, the driving pressure continues to increase, and the water saturation also decreases (Figure 6 ⑥-⑪). The core driving pressure increases from 0.5 MPa to 2 MPa, and the water saturation drops from 76% to 60%, the reduction value is 16%, and the water content of the core decrease uniformly in the whole core. Analysis suggests that in the displacement process that, with the driving pressure increases, there is one effect witch the water in smaller pores is driven by high-pressure

Preprints (www.preprints.org) | NOT PEER-REVIEWED | Posted: 21 March 2023 doi:10.20944/preprints202303.0358.v1

gas, and there is also one effect witch flowing gas carry the water go out from core. The carry effect generally reduces the water saturation by about 10% by analysis of sample A25 (Figure 7d), so the increase of the driving pressure can produce a water saturation drop of about 5%. It can be seen that when the natural gas completely go pass the core, the water saturation reduce, produced by the carry effect is about 2 times greater than that of the pressure increase.

4.3. Characters of trap charging

Trap accumulation is mainly an episodic charging process, even one pulse of episodic, it mainly 0.01-0.1Ma. Therefore, at the beginning of episodic charging, it is a rapid charging process, the charging pressure is high, charge power is mainly controlled by source rock, and the charging time is short, which is suitable for modeling of Centrifugal - Nuclear Magnetic Resonance experiment. When the charging pulse is mid-late period, the charging pressure is small, power is mainly buoyancy, and the charging time is longer, it is suitable to use the Semi-Permeable Baffle experiment to simulate.

(1) Rapidly trap charging

The centrifugal modeling is most suitable for the short-term gas charging process at the initial stage of episodic charging. The mid-late episodic charging is suitable for Semi-Permeable Baffle charging model. The NMR curves of different centrifugal forces (Figure 9) show that, cores with permeability <0.1mD have almost no large pores, cores with permeability around 0.5mD are relatively close on water content of large pores and small pores, cores with permeability >1mD has a very high water content of large pores. After centrifugation, the water saturation and permeability have a good relationship, and the permeability is higher, the water saturation is lower after centrifugation (Figure 12). The results of Cen-NMR experiments prove that the short-term rapid charging is completely affected by the physical properties of the rock (Figure 12).

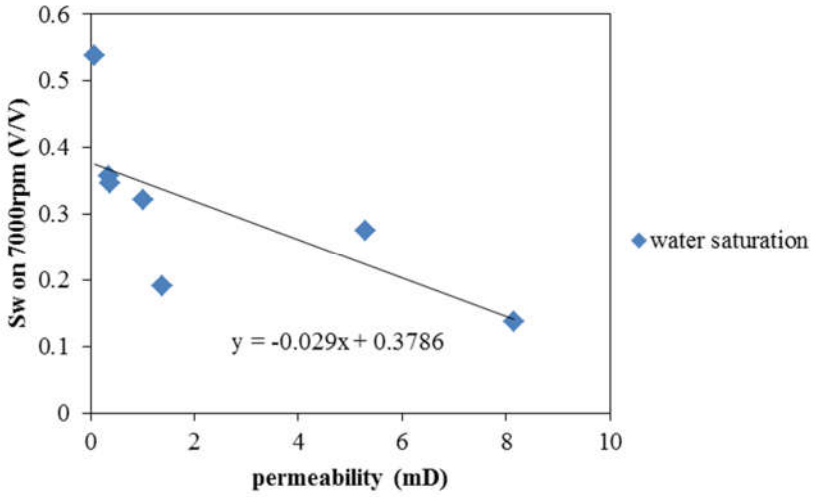

Figure 12. Relationship between rock permeability and water saturation after centrifugation.

The water saturation decrease quickly when the centrifugal force is lower than 0.8 MPa, and decline slowly if it is above 0.8 MPa (figure 9d). When the centrifugal force is above 2MPa, it is difficult to judge the change trend of water saturation due to experimental limitations. However, according to the curve extension of A7 and A45 samples, it can be seen that the water saturation of samples with higher permeability will not change as the pressure increases. For samples with lower permeability, the water saturation will still decrease as the centrifugal force increases. This shows that the rapid charging of the trap can completely fill at a about 2MPa, if the reservoir is good physical properties.

(2) Slowly trap charging

Preprints (www.preprints.org) | NOT PEER-REVIEWED | Posted: 21 March 2023 doi:10.20944/preprints202303.0358.v1

1. Time factor

The main permeability of the reservoirs in the study area is about 0.1-10mD, there are exist obviously Gas Water Contact. The charging pressure of the gas trap is calculated according to the gas-water density difference.

$$P = （\rho_w - \rho_g）g\Delta h \quad （2）$$

There, P - trap charging power, MPa; ρ_w - formation water density, g/cm3; ρ_g - natural gas density under formation conditions, g/cm3; g - gravitational acceleration, N/m; Δh - depth between gas-water contact and measuring point, km.

According to the formation conditions of the study area, the natural gas density is generally 0.2g/cm^3. The height of the gas column of mainly gas reservoirs is 150-200m. The maximum charging pressure of the reservoir top is about 1.3-1.6MPa, and the max SPB charging pressure is the 1.4MPa, which is similar with the maximum charging power of the reservoir in the study area. Even the equilibrium time for the semi-permeable charging modeling is very long, there is still a huge gap compared with the historical period of charging geology.

The gas water contact drilled in Well A-4 is about 3550m, the gas water contact is obvious, and the water saturation at about 3510m is 40%-55% by sealed cores measure (Table 2). According to the charging pressure cause by the difference in gas/water density, the charging pressure in a small area above the gas water contact is very small, only about 0.2MPa. The water saturation of SPB experimental modeling is 80%-90%, which is huge gap between that of sealed core test. This indicates that the time factor is the most important factor to control the water saturation of the reservoir. On the contrary, the pressure factor in the modeling experiment has almost negligible influence on the water saturation.

Table 2. Water saturation data of airtight coring of Huagang formation in well A-4.

well	depth m	rock density g/cm^3	Porosity %	Permeability mD	Sw of sealed cores %
A-4	3507.1	2.38	10.3	4.6	52.3
A-4	3507.4	2.35	11.2	6.5	50.8
A-4	3507.66	2.34	11.7	12.2	47.6
A-4	3509.53	2.44	7.8	0.28	61.3
A-4	3510.01	2.36	10.6	1.5	42.8
A-4	3510.41	2.38	9.9	1.2	47.6
A-4	3510.76	2.39	9.6	0.95	52.3
A-4	3511.13	2.40	9.2	0.92	56.4
A-4	3511.39	2.37	10.3	0.63	43.5
A-4	3511.71	2.42	8.4	0.65	55.0
A-4	3512.11	2.39	9.5	1.0	49.9
A-4	3512.38	2.55	4.2	0.06	37.1
A-4	3512.78	2.34	11.4	2.5	40.1
A-4	3513.1	2.39	9.5	1.7	49.7
A-4	3513.43	2.36	10.5	2.4	48.5
A-4	3514.03	2.36	10.6	2.7	49.3
A-4	3514.45	2.37	10.6	1.1	48.6
A-4	3514.61	2.38	10.8	1.7	51.9

Considering the time factor, even the charging pressure is low, the reservoir can still reach a high gas saturation. Therefore, for traps with relatively good physical properties, the water saturation of the reservoir above the gas water contact reaches the minimum. The conclusion that the charging pressure affects the water saturation in experimental modeling is not suitable for the slow charging of traps in the geological accumulation.

Preprints (www.preprints.org) | NOT PEER-REVIEWED | Posted: 21 March 2023 doi:10.20944/preprints202303.0358.v1

From the experimental modeling and sealed cores analysis, the slow trap accumulation is only affected by the time factor.

2. Final water saturation

Even though the SPB charging experiment modeling cannot truly describe the trap accumulation process, the minimum water saturation obtained by the SPB is very matched with the sealed core data.

According to the SPB charging modeling experiment, when the charging pressure is about 1.2MPa, the water saturation of the reservoir is basically stable, the increase of charging pressure will no longer cause the water saturation to decrease (Figure 8 a, b, c), and the water saturation is basically maintained at about 40%-50%, it shows that the water saturation of 40%-50% is the lowest water saturation that the reservoir can reach, that is, the maximum gas saturation of the study area is 50%-60%. The water saturation of the sealed cores measurement in well A-4 is basically 40%-55% (table 2), which matches the final water saturation of 40%-50% obtained by the SPB experimental modeling (figure 12).

The water saturation data of the sealed cores is negatively correlated with the rock physical properties, but the correlation is poor, which also shows that the physical properties have little influence on the water saturation of the reservoir, and are greatly affected by the charging time.

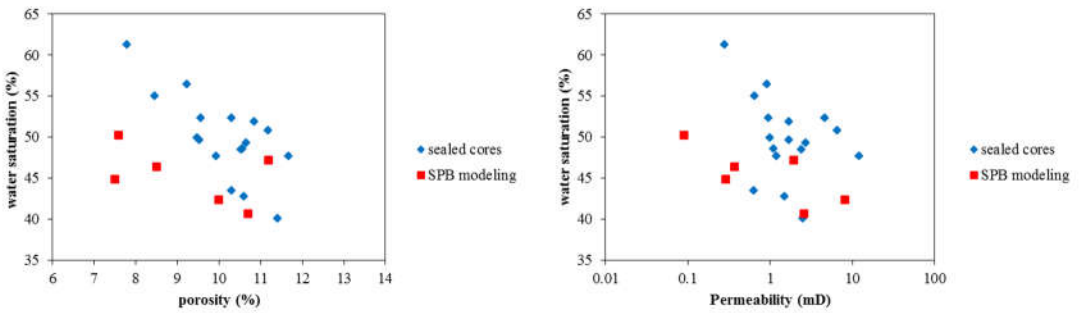

Figure 13. Comparison of final water saturation between sealed cores and SPB modeling.

5. Conclusion

(1) There is an start-up pressure gradient in the sandstone migration layer. The main effect of the charging of the migration layer is driving effect and carrying effect. The driving front of migration layer is basically flat. The start-up pressure with a permeability of 0.3mD is 0.6MPa, the start-up pressure gradient is 0.17MPa/cm, and the length of the driving front observed in the modeling experiment is about 1-1.5cm. The driving effect can reduce the water saturation to 70%-80%, and the carry effect makes the water saturated also reduced by 5%-10%, so the carry effect cannot be ignored.

(2) The rapid charging of the trap is only affected by the physical properties of the reservoir, the porosity and permeability is better, the final water saturation will be lower. Before the centrifugal force is 0.8 MPa, the water saturation decreases rapidly, and after 0.8 MPa, the water saturation decreases slowly.

(3) The water saturation of slow trap charging is stable at 40%-50%, which has little to do with the physical properties and charging power. The semi-permeable baffle charging experiment matches the water saturation data of the sealed core measure.

Acknowledgement: This paper was funded by the National Science and Technology Major Project (No. 2016ZX05027-002-001), thanks to the State Key Laboratory of Oil and Gas and Resource Exploration, China University of Petroleum (Beijing), and Professor Huang for his guidance in writing the paper, Dr. Zhang, Dr. Dong, Dr. Li, thanks to the project team members who provided assistance in writing the paper.

Preprints (www.preprints.org) | NOT PEER-REVIEWED | Posted: 21 March 2023 doi:10.20944/preprints202303.0358.v1

Reference

Arogun, O., Nwosu, C., 2011. Capillary pressure curves from nuclear magnetic resonance log data in a deepwater turbidite nigeria field — a comparison to saturation models from scal drainage capillary pressure curves. Society of Petroleum Engineers. https://doi.org/10.2118/150749-MS.

Chen, S.D., Tang, D.Z., Tao, S., Ji, X.Y., Xu, H., 2019. Fractal analysis of the dynamic variation in pore-fracture systems under the action of stress using a low-field NMR relaxation method: an experimental study of coals from western guizhou in china. Journal of Petroleum ence and Engineering, 173, 617-629.

Daigle, H., Johnson, A.. 2015. Combining mercury intrusion and nuclear magnetic resonance measurements using percolation theory. Transport in Porous Media, 111(3), 1-11.

Duan, W., Luo, C., Lou, Z., Liu, J., Jin, A., Zhu, , 2017. Diagenetic differences caused by the charging of natural gases with various compositions - a case study on the lower zhuhai formation clastic reservoirs in the wc-a sag, the pearl river mouth basin. Marine and Petroleum Geology. 81, 149-168.

Eslami, M. , Kadkhodaie-Ilkhchi, A. , Sharghi, Y. , & Golsanami, N. . 2013. Construction of synthetic capillary pressure curves from the joint use of NMR log data and conventional well logs. Journal of Petroleumence & Engineering, 111, 50-58.

Feng, C., Guimares, A.S., Ramos, N., Sun, L., Janssen, H., 2020. Hygric properties of porous building materials (vi): a round robin campaign. Building and Environment, 185, 107242.

Glorioso, J.C., Aguirre, O., Piotti, G., Mengual, J.F., 2003. Deriving Capillary Pressure and Water Saturation from NMR Transversal Relaxation Times. Society of Petroleum Engineers. https://doi.org/10.2118/81057-MS.

Gu, J., Jeong, Y.J., Na, J.Y., Seon, J.K., Kang, K., 2020. Application of semi-permeable membrane for a scaffold in a nature-mimicking vascular system. Journal of Membrane Science, 611, 118384.

Guo, X., Huang, Z., Zhao, L., Han, W., Ding, C., Sun, X., 2019. Pore structure and multi-fractal analysis of tight sandstone using MIP, NMR and NMRC methods: a case study from the kuqa depression, china. Journal of Petroleum Science & Engineering. 178, 544–558

Li, Y.B., Zhang, Y.Q., Luo, C., Gao, H., Li, K., Xiao, Z.R., et al. 2019. The experimental and numerical investigation of in situ re-energization mechanism of urea-assisted steam drive in superficial heavy oil reservoir. Fuel, 249(AUG.1), 188-197.

Lu, T., Li, Z.M., Li, S.Y., Wang, P., Wang, Z.Z., Liu, S.Q., 2016. Enhanced heavy oil recovery after solution gas drive by water flooding. Journal ofPetroleumScienceandEngineering, 137, 113-124.

Lysova, A.A., Garnier, A.V., Hardy, E.H., Reimert, R., Koptyug, I.V., 2011. The influence of an exothermic reaction on the spatial distribution of the liquid phase in a trickle bed reactor: direct evidence provided by nmr imaging. Chemical Engineering Journal. 173, 552-563.

Masri, W., Shapiro, A.. 2021. Experimental determination of relative permeabilities and critical gas saturations under solution-gas drive. Journal of Petroleum Science and Engineering, 202, 108509.

Niroomand, S., Fauchoux, M.T., Simonson, C.J., 2019. Evaluation of the frost properties on a semipermeable membrane. International Journal of Heat and Mass Transfer, 133(APR.), 435-444.

Shao, X., Pang, X., Jiang, F., Li, L., Huyan, Y., D Zheng., 2017. Reservoir characterization of tight sandstones using nuclear magnetic resonance and incremental pressure mercury injection experiments: implication for tight sand gas reservoir quality. Energy & Fuels, acs.energyfuels.7b01184.

Wang, X.Q., Sun, L., Zhu, R.K., et al. 2015. Application of charging effects in evaluating storage space of tight reservoirs: A case study from Permian Lucaogou Formation in Jimusar sag, Junggar Basin, NW China[J]. Shiyou Kantan Yu Kaifa/Petroleum Exploration and Development, 42(4):516-524.

Wang, Y., Hou, J.R. , Tang, Y., Song, Z.J., 2019. Effect of vug filling on oil-displacement efficiency in carbonate fractured-vuggy reservoir by natural bottom-water drive: a conceptual model experiment. Journal of Petroleum Science and Engineering, 174, 1113-1126.

Wang, J., Fu, J., Xie, J., Wang, J.. 2020. Quantitative characterisation of gas loss and numerical simulations of underground gas storage based on gas displacement experiments performed with systems of small-core devices connected in series. Journal of Natural Gas Science and Engineering. 81, 103495.

Wang, M., Yang, Y., Miao, G., Zhou, X.. 2021. An experimental study on coal damage caused by two-phase displacement of co2-alkaline solution. Journal of Natural Gas Science and Engineering, 93(2), 104034.

Wen, Y. , Qu, M. , Hou, J. , Liang, T. , Yuan, N. . 2019. Experimental study on nitrogen drive and foam assisted nitrogen drive in varying-aperture fractures of carbonate reservoir. Journal of Petroleum Science and Engineering, 180.

Xu, Z.J., Liu, L.F., Wang, T.G., Wu, K.J., Gao, X.Y., et al. 2017. Application of fluid inclusions to the charging process of the lacustrine tight oil reservoir in the triassic yanchang formation in the ordos basin, china. Journal of Petroleum Science & Engineering, 149, 40-55.

Xue, D. J., Liu, Y.T., Zhou, J., Sun, X.T., 2019. Visualization of helium-water flow in tight coal by the low-field nmr imaging: an experimental observation. Journal of Petroleum Science and Engineering, 188, 106862.

Zheng, M., Li, J., Wu, X., Li, P., Wang, W., Wang, S. , et al. 2016. Physical modeling of oil charging in tight reservoirs: a case study of permian lucaogou formation in jimsar sag, junggar basin, nw china. Petroleum Exploration and Development, 43(2), 241-250.

Zuo, J. Y. , Mullins, O. C. , Achourov, V. , Pfeiffer, T. , Pan, S. , & Wang, K. , et al. 2017. Fluid distributions during light hydrocarbon charges into oil reservoirs using multicomponent maxwell-stefan diffusivity in gravitational field. Fuel, 209, 211-223.